JCTC Journal of Chemical Theory and Computation

Article

Cite This: J. Chem. Theory Comput. 2018, 14, 3656−3666

pubs.acs.org/JCTC

Linked-Cluster Formulation of Electron−Hole Interaction Kernel in Real-Space Representation without Using Unoccupied States

Michael G. Bayne, Jeremy A. Scher, Benjamin H. Ellis, and Arindam Chakraborty*

Department of Chemistry, Syracuse University, Syracuse, New York 13244 United States

Supporting Information

ABSTRACT: Electron−hole or quasiparticle representation plays a central role in describing electronic excitations in many-electron systems. For charge-neutral excitation, the electron−hole interaction kernel is the quantity of interest for calculating important excitation properties such as optical gap, optical spectra, electron−hole recombination, and electron−hole binding energies. The electron−hole interaction kernel can be formally derived from the density−density correlation function using both Green's function and time-dependent density functional theory (TDDFT) formalism. The accurate determination of the electron−hole interaction kernel remains a significant challenge for precise calculations of optical properties in the GW+BSE formalism. From the TDDFT perspective, the electron−hole interaction kernel has been viewed as a path to systematic development of frequency-dependent exchange−correlation functionals. Traditional approaches, such as many-body perturbation theory formalism, use unoccupied states (which are defined with respect to Fermi vacuum) to construct the electron−hole interaction kernel. However, the inclusion of unoccupied states has long been recognized as the leading computational bottleneck that limits the application of this approach for larger finite systems. In this work, an alternative derivation that avoids using unoccupied states to construct the electron−hole interaction kernel is presented. The central idea of this approach is to use explicitly correlated geminal functions for treating electron−electron correlation for both ground and excited state wave functions. Using this ansatz, it is derived using both diagrammatic and algebraic techniques that the electron−hole interaction kernel can be expressed only in terms of linked closed-loop diagrams. It is proved that the cancellation of unlinked diagrams is a consequence of linked-cluster theorem in real-space representation. The electron−hole interaction kernel derived in this work was used to calculate excitation energies in many-electron systems, and results were found to be in good agreement with the EOM-CCSD and GW+BSE methods. The numerical results highlight the effectiveness of the developed method for overcoming the computational barrier of accurately determining the electron−hole interaction kernel to applications of large finite systems such as quantum dots and nanorods.

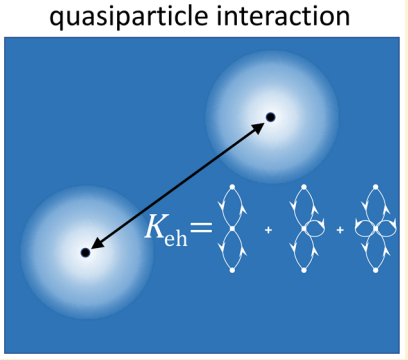

1. INTRODUCTION

The concept of electron−hole or particle−hole quasiparticle formulation is central to the treatment of electronically excited states in many-electron systems. The electron−hole picture represents excitation from the Fermi vacuum and constitutes the zeroth-order treatment of electronic excitation. In addition, the electron−hole excitation is used extensively in various formulations for treating electron correlation for both ground and electronically excited states.[1]

For charge-neutral excitations, the accurate treatment of electron−hole interaction is extremely important.[2−5] For example, in the Bethe−Salpeter (BSE) approach, the electron−hole interaction kernel is used for calculations of excitation energies.[6−14] The electron−hole interaction kernel can be obtained using both many-body perturbation theory (MBPT)[1,15−21] and time-dependent density functional theory (TDDFT).[1,22−26] In both of these approaches, it has been shown convincingly that accurate determination of electron−hole screening is crucial for the accurate calculation of excitation energy.

The overarching objective of this work is the determination of electron−hole screening in excited states without using unoccupied states. Although the BSE approach has been very successful in predicting the optical spectra of periodic solids and finite-size clusters, it is restricted by the computational effort it takes to construct the electron−hole interaction kernel. In a traditional approach, the construction of the electron−hole interaction kernel requires knowledge of a large number of virtual or unoccupied states. This feature puts severe limitations on the applicability of the BSE and other methods that rely on electron−hole screening for treating large finite-size clusters such as quantum dots and rods. In this work, we present the derivation of the electron−hole interaction kernel that does not require unoccupied states. This is a real-space formulation that uses the connection between electron−hole screening and electron−electron correlation to avoid unoccupied states in the construction of the electron−hole interaction kernel. A similar strategy has also been developed by Nichols and Rassolov using real-space electron correlator approach.[27] We anticipate that using such a kernel will result in significant reduction in

Received: February 4, 2018
Published: May 21, 2018

DOI: 10.1021/acs.jctc.8b00123
J. Chem. Theory Comput. 2018, 14, 3656−3666

the cost of the BSE method. This work is also relevant in the TDDFT formulation with respect to the construction of the effective exchange−correlation functional.[5] Because the derivation presented here is using real-space as opposed to occupation-number space, we expect this approach is much more amenable to the development of exchange−correlation functionals.

Recently, in a series of articles, Galli and co-workers have developed the WEST method that addresses the issue of removing contributions of unoccupied states from the GW and BSE equations.[28−30] This method relies on projecting out non-contributing terms from the dielectric matrix. The derivation presented here uses a strategy different than the one used for the WEST method. First, this method is derived from the equation-of-motion approach developed by Simons et al.,[31−37] Cederbaum et al.,[38−42] and Yeager and McKoy.[43−50] This method calculates the electron−hole interaction kernel directly for charge-neutral excitations without requiring the construction or knowledge of the one-particle Green's function. This derivation also does not assume that it is a post-DFT procedure and in general can be applied to both Hartree−Fock and ground state DFT formulations. In this work, the bare electron and hole quasiparticles are defined with respect to the Fermi vacuum and are constructed from single-particle states of an effective one-electron Hamiltonian. We present two equivalent derivations of the electron−hole interaction kernel. In the first derivation, we show a compact derivation using Hugenholtz diagrams in section 2, and we present the derivation using algebraic representation in Appendix A.

An important connection between electron−hole screening and electron−electron correlation is that electron−hole screening is a consequence of electron−electron correlation. For example, in a hypothetical many-electron system that lacks electron−electron correlation, the electron−hole interaction can be described exactly as the bare Coulomb interaction. Hence, treatment of electron−electron correlation is very important for studying electron−hole interaction. In this work, we use the two-body geminal operator, G, for treating electon−electon correlation,

$$\Psi = G\Phi_0 \tag{1}$$

where G is a real-space operator that depends explicitly on the electron−electron separation distance, r_{12}. An explicitly correlated operator with r_{12} dependence can be used to provide a better description of the many-electron wave function near the electron−electron coalescence point.[51] For example, both variational Monte Carlo[52,53] and transcorrelated Hamiltonian[54,55] are methods that use the ansatz in eq 1 for the many-electron wave function. The connection between the explicitly correlated wave function (eq 1) and configuration interaction (CI) can be seen by applying the identity operator on the correlated wave function (eq 2),

$$\sum_{k=0}^{\infty} |\Phi_k\rangle\langle\Phi_k| = I \tag{2}$$

and substituting in eq 1,

$$|\Psi\rangle = IG|\Phi_0\rangle = \left[\sum_{k=0}^{\infty} |\Phi_k\rangle\langle\Phi_k|\right] G|\Phi_0\rangle \tag{3}$$

Equation 3 is an infinite-order CI expansion which is shown in eq 4,

$$|\Psi\rangle = \sum_{k=0}^{\infty} c_k^G |\Phi_k\rangle \tag{4}$$

where the expansion coefficients $c_k^G = \langle\Phi_k|G|\Phi_0\rangle$ are constrained to be a functional of G. The inclusion of this explicit r_{12} dependence in the wave function has been used since the early days of quantum mechanics to achieve accurate ground state energies. Slater[56,57] and Hylleraas[58,59] first used the explicitly correlated wave function calculating the ground state energy in helium atom in 1929. Since then and especially within the past 30 years, the inclusion of explicit correlation has been implemented in various methods such as variational Monte Carlo,[52,53] transcorrelated Hamiltonian,[54,55,60−62] explicitly correlated Hartree−Fock,[63−72] geminal augmented MCSCF,[73] the electronic mean field configuration interaction method,[74] and the strongly orthogonal geminal method.[75,76] The field of explicitly correlated method has been recently reviewed by various authors.[77−80]

2. THEORY

In this section, we present the derivation of the electron−hole interaction kernel using Hugenholtz diagrams. We start by defining a zeroth-order Hamiltonian,

$$H_0 = \sum_i^N \left[\frac{-\hbar^2}{2m}\nabla_i^2 + v_{\text{ext}}(i) + v_{\text{eff}}(i)\right] \tag{5}$$

where v_{eff} is a one-particle effective potential for which the eigenvalues and eigenfunctions of H_0 can be computed exactly. This derivation does not require a specific form of the effective potential, and v_{eff} can be obtained using various methods such as Hartree−Fock (v_{HF}), KS-DFT (v_{KS}), pseudopotential (v_{ps}), or empirical model potential (v_{emp}). The ground and excited electronic states in the non-interacting system (described by H_0) are represented by Φ_0 and Φ_i^a, respectively.

$$H_0|\Psi_0\rangle = E_0^{(0)}|\Phi_0\rangle \tag{6}$$

$$H_0|\Phi_i^a\rangle = E_{ia}^{(0)}|\Phi_i^a\rangle \tag{7}$$

The excitation energy in the non-interacting system is represented by ω_{X}^0 and is calculated from the difference in the eigenvalues of the one-particle Hamiltonian,

$$\omega_{\text{X}}^0 = (E_{ia}^{(0)} - E_0^{(0)}) = \epsilon_a - \epsilon_i \tag{8}$$

Using the effective potential, we define the residual electron−electron interaction operator W which is the part of the Coulomb operator not included in the effective potential. Mathematically, W is a two-body operator which is expressed as,

$$W = \sum_{i<j} w(i,j) = \sum_{i<j}^{N} r_{ij}^{-1} - \sum_i^N v_{\text{eff}}(i) \tag{9}$$

The many-electron Hamiltonian is defined as

$$H = H_0 + W \tag{10}$$

and the corresponding ground and excited state wave functions are defined as

$$H|\Psi_0\rangle = E_0|\Psi_0\rangle \tag{11}$$

$$H|\Psi_{\text{X}}\rangle = E_{\text{X}}|\Psi_{\text{X}}\rangle \tag{12}$$

DOI: 10.1021/acs.jctc.8b00123
J. Chem. Theory Comput. 2018, 14, 3656−3666

where the subscript "X" is used to represent excited state. The excitation energy in the correlated system is analogously defined as

$$\omega_X = (E_X - E_0) \tag{13}$$

The ground and excited state correlated wave functions are normalized using the following intermediate normalization condition,

$$\langle \Phi_0 | \Psi_0 \rangle = \langle \Phi_i^a | \Psi_X \rangle = 1 \tag{14}$$

In this derivation, we assume that the ansatz for the correlated ground state, Ψ_0, and the excited state, Ψ_X, wave functions are defined with respect to their corresponding uncorrelated wave function and correlation operator, G. The expressions for the correlated ground and excited state wave functions are given by

$$\Psi_0 = G_0 \Phi_0 \tag{15}$$

$$\Psi_X = G_X \Phi_i^a \tag{16}$$

where the correlation operator is a two-body operator with the following form,

$$G_0 = \sum_{i<j}^{N} g_0(i, j) \tag{17}$$

$$G_X = \sum_{i<j}^{N} g_X(i, j) \tag{18}$$

The derivation presented here is general and does not depend on the choice of $g(1,2)$. However, practical implementation of this method requires specific choice of $g(1,2)$, and the functional form used in this work will be discussed in Results and Discussion.

The goal of this derivation is to find the relationship between the excitation energies of the correlated (ω_X) and the uncorrelated (ω_X^0) systems. We start by left-multiplying the eigenvalue equation for the correlated system (eq 11) by the uncorrelated bra-vectors, shown as follows,

$$\langle \Phi_0 | H | \Psi_0 \rangle = E_0 \langle \Phi_0 | \Psi_0 \rangle \tag{19}$$

$$\langle \Phi_i^a | H | \Psi_X \rangle = E_X \langle \Phi_i^a | \Psi_X \rangle \tag{20}$$

Using intermediate normalization (eq 14) and expanding the Hamiltonian (eq 10) we get

$$\langle \Phi_0 | [H_0 + W] | \Psi_0 \rangle = E_0 \tag{21}$$

$$\langle \Phi_i^a | [H_0 + W] | \Psi_X \rangle = E_X \tag{22}$$

Operating on the bra-vector with H_0 gives

$$E_0^{(0)} + \langle \Phi_0 | W | \Psi_0 \rangle = E_0 \tag{23}$$

$$E_{ia}^{(0)} + \langle \Phi_i^a | W | \Psi_X \rangle = E_X \tag{24}$$

Subtracting the two equations gives

$$E_X - E_0 = (E_{ia}^{(0)} - E_0^{(0)}) + \langle \Phi_i^a | W | \Psi_X \rangle - \langle \Phi_0 | W | \Psi_0 \rangle \tag{25}$$

Using eq 8 and eq 13, the above equation can be used to relate the excitation energies of the correlated system with the excitation energies of the uncorrelated system,

$$\omega_X = \omega_X^0 + \langle \Phi_i^a | W | \Psi_X \rangle - \langle \Phi_0 | W | \Psi_0 \rangle \tag{26}$$

Substituting eq 15 and eq 16 into eq 26, we arrive at the following expression of the excitation energy,

$$\omega_X = \omega_X^0 + \langle 0 | \{i^\dagger a\} W G_X \{a^\dagger i\} | 0 \rangle - \langle 0 | W G_0 | 0 \rangle \tag{27}$$

where

$$|\Phi_0\rangle \equiv |0\rangle \tag{28}$$

$$|\Phi_i^a\rangle \equiv \{a^\dagger i\} |0\rangle \tag{29}$$

We recognize that the expression in eq 27 involves evaluation of the vacuum expectation value of operators. Using Wick's contraction theorem, we can immediately conclude than only fully contracted terms will contribute to the above expression,[15] because as shown below, the expectation value of uncontracted terms with respect to the Fermi vacuum will have zero contribution,

$$\langle 0 | X | 0 \rangle = \langle 0 | X^\dagger | 0 \rangle = 0$$
$$(X \text{ is any second-quantized operator}) \tag{30}$$

Therefore, we can write the following expression,

$$\langle 0 | \{i^\dagger a\} W G_X \{a^\dagger i\} | 0 \rangle = \langle 0 | \{i^\dagger a\} W G_X \{a^\dagger i\} | 0 \rangle_{FC} \tag{31}$$

$$\langle 0 | W G_0 | 0 \rangle = \langle 0 | W G_0 | 0 \rangle_{FC} \tag{32}$$

where as the subscript "FC" implies, only fully contracted terms are evaluated in the above expression. The set of all fully contracted terms will contain both linked and unlinked terms and will be discussed later. Substituting eq 31 and eq 32 into eq 27 gives

$$\omega_X = \omega_X^0 + \langle 0 | \{i^\dagger a\} W G_X \{a^\dagger i\} | 0 \rangle_{FC} - \langle 0 | W G_0 | 0 \rangle_{FC} \tag{33}$$

The first term in the above expression represents the excitation energy in the zeroth-order Hamiltonian. The second term contains the electron−hole interaction terms. The expression of this term in terms of electron and hole indices can be obtained using diagrammatic techniques, and in this work we will use the Hugenholtz diagrams[15,72,81] for a compact representation of the diagrams. To derive expression for the second term in eq 33, we note that operator WG_X is a product of two, two-body operators W and G_X. Therefore, this product can be expanded into a sum of two-body, three-body, and four-body operators[72] by substituting the definitions of W and G_X from eq 9 and eq 18. The resulting expansion is shown below,

$$WG_X = \sum_{i<j} w(i, j) \times \sum_{i<j} g_X(i, j) \tag{34}$$

$$= \sum_{i<j} \kappa_2^X(i, j) + \sum_{i<j<k} \kappa_3^X(i, j, k) + \sum_{i<j<k<l} \kappa_4^X(i, j, k, l) \tag{35}$$

$$= \Omega_2^X + \Omega_3^X + \Omega_4^X \tag{36}$$

The expression for $(\kappa_2^X, \kappa_3^X, \kappa_4^X)$ can be obtained using the operators of the complete symmetric group $\mathcal{S}_N$, for example,

$$\kappa_2^X(1,2) = w(1,2)\, g_X(1,2) \tag{37}$$

$$= \frac{1}{2!}[w(1,2)\, g_X(1,2) + w(2,1)\, g_X(2,1)] \tag{38}$$

$$= \frac{1}{2!} \sum_{P_\alpha \in \mathcal{S}_2} P_\alpha [w(1,2)\, g(1,2)] \tag{39}$$

where P_α is the permutation operator in $\mathcal{S}_N$ that permutes the symbols $[1,2]$ to one of the $N!$ arrangements,

DOI: 10.1021/acs.jctc.8b00123
J. Chem. Theory Comput. 2018, 14, 3656−3666

$$P_\alpha[1,2] = [\pi_1, \pi_2] \tag{40}$$

Therefore,

$$\kappa_3^X(1,2,3) = \frac{1}{3!}\sum_{P_\alpha \in S_3} P_\alpha[w(1,2)\, g_X(2,3)] \tag{41}$$

$$\kappa_4^X(1,2,3,4) = \frac{1}{4!}\sum_{P_\alpha \in S_4} P_\alpha[w(1,2)\, g_X(3,4)] \tag{42}$$

We note that the above expression guarantees that operators are completely symmetric with respect to the permutation of electronic coordinates. We have similar expressions for the WG_0 term,

$$WG_0 = \sum_{i<j} w(i,j) \sum_{i<j} g_0(i,j) \tag{43}$$

$$= \sum_{i<j} \kappa_2^0(i,j) + \sum_{i<j<k} \kappa_3^0(i,j,k) + \sum_{i<j<k<l} \kappa_4^0(i,j,k,l) \tag{44}$$

$$= \Omega_2^0 + \Omega_3^0 + \Omega_4^0 \tag{45}$$

The evaluation of the matrix elements of operators $\langle 0|\{i^\dagger a\}\Omega\{a^\dagger i\}|0\rangle$ can then be performed using second-quantized algebra. We note that matrix element is of the general form $\langle 0|\cdots|0\rangle$ and is an expectation value expression with respect to the vacuum state. This allows us to apply Wick's contraction theorem and conclude that only fully contracted terms will have nonzero contributions to the matrix elements. The expressions resulting from Wick's contraction are represented diagrammatically for a compact representation and are presented in Figure 1. An equivalent but longer derivation using algebraic representation is presented in Appendix A, and description of Hugenholtz diagrams are presented in the Supporting Information.[81] Specifically, fully contracted terms from $\langle 0|WG_0|0\rangle$ are represented by diagrams D_1, D_2, and D_3 in panel A of Figure 1,

$$\langle 0|\Omega_2^0|0\rangle_{FC} = D_1 \tag{46}$$

$$\langle 0|\Omega_3^0|0\rangle_{FC} = D_2 \tag{47}$$

$$\langle 0|\Omega_4^0|0\rangle_{FC} = D_3 \tag{48}$$

substituting

$$\langle 0|WG_0|0\rangle_{FC} = \langle 0|\Omega_2^0|0\rangle_{FC} + \langle 0|\Omega_3^0|0\rangle_{FC} + \langle 0|\Omega_4^0|0\rangle_{FC} \tag{49}$$

$$= D_1 + D_2 + D_3 \tag{50}$$

These diagrams do not have any particle−hole lines because these expressions only involve occupied states which are represented by closed loops in the diagrams. Therefore, as shown in Figure 1, all the terms are obtained from linked diagrams,

$$\langle 0|WG_0|0\rangle_{FC} = \langle 0|WG_0|0\rangle_L \tag{51}$$

The equivalent algebraic derivation of eq 51 using second-quantized operators is presented in Appendix A.

The fully contracted terms from $\langle 0|WG_X|0\rangle$ are represented by diagrams D_4, ..., D_{18} in panel B of Figure 1,

$$\langle 0|\{i^\dagger a\}\Omega_2^X\{a^\dagger i\}|0\rangle_{FC} = D_4 + D_7 + D_{10} + D_{13}D_{16} \tag{52}$$

$$\langle 0|\{i^\dagger a\}\Omega_3^X\{a^\dagger i\}|0\rangle_{FC} = D_5 + D_8 + D_{11} + D_{14}D_{17} \tag{53}$$

$$\langle 0|\{i^\dagger a\}\Omega_4^X\{a^\dagger i\}|0\rangle_{FC} = D_6 + D_9 + D_{12} + D_{15}D_{18} \tag{54}$$

We note that the diagram pairs (D_{13},D_{16}), (D_{14},D_{17}), and (D_{15},D_{18}) form the set of all unlinked diagrams. However, analysis of the bubble diagrams D_{16}, D_{17}, and D_{18} reveals that all these diagrams refer to the same electron−hole pair and are exactly equal to 1. Algebraically, they represent the following Wick's contraction,

$$D_{16} = D_{17} = D_{18} = \langle 0|\{i^\dagger a\}\{a^\dagger i\}|0\rangle = 1 \tag{55}$$

Substituting eq 55 in eq 52, we get

$$\langle 0|\{i^\dagger a\}\Omega_2^X\{a^\dagger i\}|0\rangle_{FC} = D_4 + D_7 + D_{10} + D_{13} \tag{56}$$

$$\langle 0|\{i^\dagger a\}\Omega_3^X\{a^\dagger i\}|0\rangle_{FC} = D_5 + D_8 + D_{11} + D_{14} \tag{57}$$

$$\langle 0|\{i^\dagger a\}\Omega_4^X\{a^\dagger i\}|0\rangle_{FC} = D_6 + D_9 + D_{12} + D_{15} \tag{58}$$

Combining all the terms in eq 56

$$\langle 0|\{i^\dagger a\}WG_X\{a^\dagger i\}|0\rangle_{FC} = D_4 + D_7 + D_{10} + D_{13} + D_5 + D_8 + D_{11} + D_{14} + D_6 + D_9 + D_{12} + D_{15} \tag{59}$$

We note that all the diagrams in the above expression are linked diagrams, therefore the left-hand side of eq 59 can be expressed solely in terms of linked terms. The summation of loop diagrams D_{13}, ..., D_{15} is equal to the vacuum expectation value of the operator,

$$D_{13} + D_{14} + D_{15} = \langle 0|WG_X|0\rangle_L \tag{60}$$

and the summation of the remaining diagrams are related to the following matrix element,

$$D_4 + \ldots + D_{12} = \langle 0|\{i^\dagger a\}WG_X\{a^\dagger i\}|0\rangle_L \tag{61}$$

where the subscript L implies that only linked diagrams are included in that expression. Therefore, we conclude that the matrix elements (summarized in panels A and B of Figure 1) consist of only linked diagrams. Combining the results from eq 60 and eq 61, we conclude that only linked diagrams contribute to the expression as shown in eq 62,

$$\langle 0|\{i^\dagger a\}WG_X\{a^\dagger i\}|0\rangle = \langle 0|\{i^\dagger a\}WG_X\{a^\dagger i\}|0\rangle_L + \langle 0|WG_X|0\rangle_L \tag{62}$$

The equivalent algebraic derivation of eq 62 using second-quantized operators is presented in Appendix A.

To obtain the expression for ω_X, we observe that the D_1...D_3 and D_{13}...D_{15} diagrams have similar structures and can be combined together into a single expression. Mathematically, substituting eq 62 in eq 27 gives the following expression for ω_X,

$$\omega_X = \omega_X^0 + \langle 0|W(G_X - G_0)|0\rangle + \langle 0|\{i^\dagger a\}WG_X\{a^\dagger i\}|0\rangle_L \tag{63}$$

The diagrammatic expression for eq 63 is given in panel C of Figure 1. An important result from this derivation is the proof that the excitation energy of the correlated system can be expressed entirely in terms of linked diagrams. The diagrammatic representation in Figure 1 implies the following expression for the excitation energy,

$$\omega_X = \omega_X^0 + D_{19} + \ldots + D_{30} \tag{64}$$

The diagrams can be related to matrix elements of the following one-body and two-body operators,

DOI: 10.1021/acs.jctc.8b00123
J. Chem. Theory Comput. 2018, 14, 3656−3666

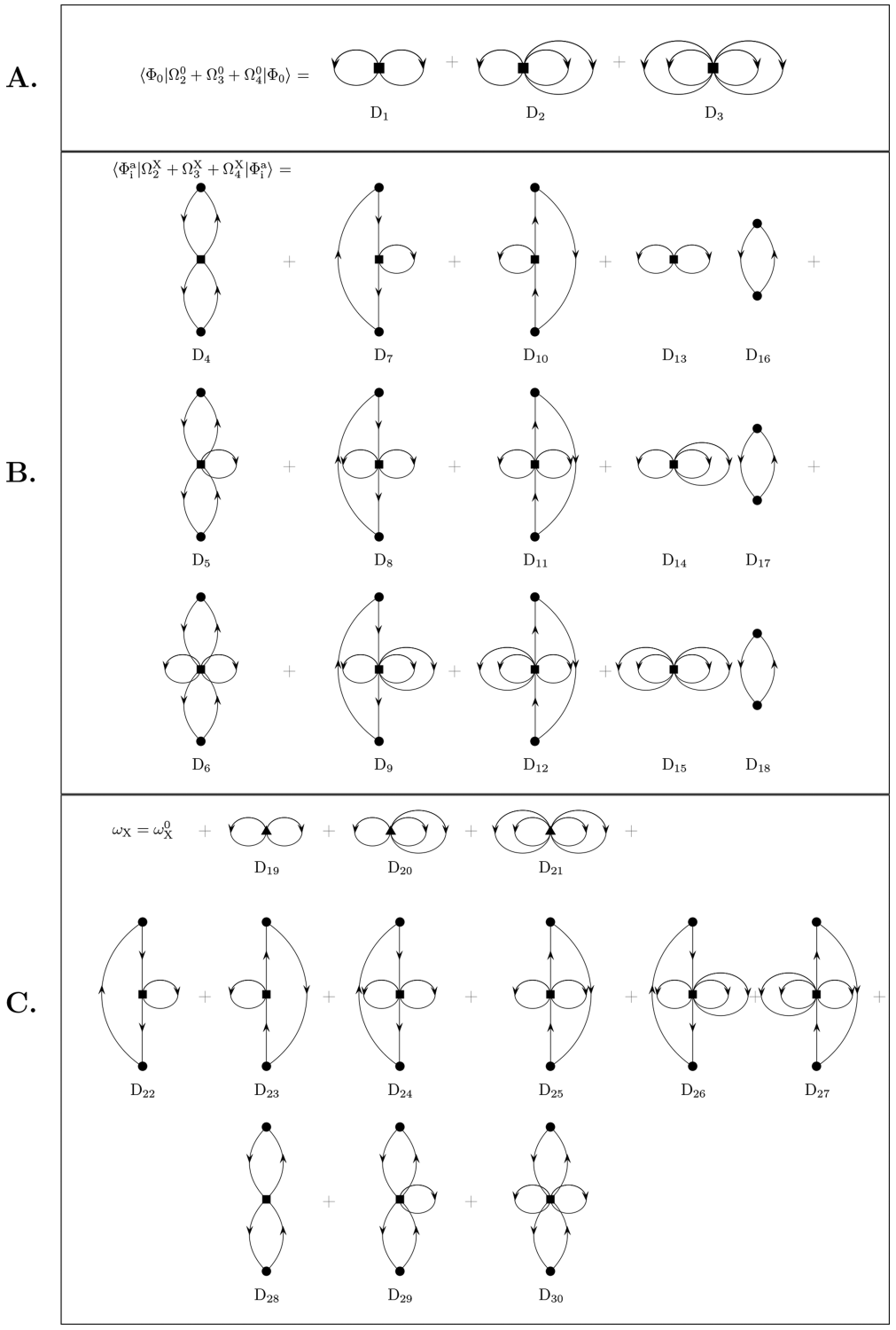

Figure 1. Derivation represented using Hugenholtz diagrams. Diagrams D_{19} through D_{21} have the operator represented by ▲, which corresponds to the operator $W(G_X-G_0)$. Diagrams with ■ represent operators κ_2^X, κ_3^X, and κ_4^X.

$$\omega_X = \omega_X^0 + \langle 0|W(G_X - G_0)|0\rangle + \langle i|U_h|i\rangle + \langle a|U_e|a\rangle + \langle ia|K_{eh}|ai\rangle \quad (65)$$

The first term, ω_X^0, in eq 65 is the excitation energy in the reference system. The remaining terms in the equation are corrections to the reference excitation energy due to the electron−electron correlation effect. The second term in eq 65 is obtained from the following combination of diagrams,

$$\langle 0|W(G_X - G_0)|0\rangle = D_{19} + D_{20} + D_{21} \quad (66)$$

In this diagrammatic representation, $D_{19} = D_8 - D_1$, $D_{20} = D_{13} - D_2$, and $D_{21} = D_{18} - D_3$, respectively. The expressions of these terms in terms of the one-particle basis functions $\{\chi_p\}$ are presented in Appendix A. This term is a vacuum expectation value and therefore does not contribute to the electron−hole interaction kernel. Because of the $W(G_X-G_0)$ term in the above expression (represented by ▲ in Figure 1), this expression

DOI: 10.1021/acs.jctc.8b00123
J. Chem. Theory Comput. 2018, 14, 3656−3666

represents the correction to the reference excitation energy, ω_X^0, due to the difference in the treatment of electron−electron correlation in the ground and excited state wave functions. In the limit where the electron−electron correlation operator for both ground and excited states are identical, the contribution from this term will be zero. The terms U_h and U_e are obtained from the following diagrams,

$$\langle i|U_h|i\rangle + \langle a|U_e|a\rangle = D_{22} + ... + D_{27} \quad (67)$$

In diagrammatic representation, $U_{e,h}$ implies that the operators are one-body operators that operate either on the quasielectron or quasihole particles. The correction to the excitation energy due to $U_{e,h}$ can be interpreted as the consequence of the renormalization of the electron and hole energy levels due to the presence of the electron−electron correlation. We note that $U_{e,h}$ depends only on the form of the electron−electron correlation operator for the excited state and not on the ground state correlator operator. The operator (■) in diagrams D_{28}, D_{29}, and D_{30} operates simultaneously on both electron and hole lines and represents the electron−hole interaction kernel,

$$\langle ia|K_{eh}|ai\rangle = D_{28} + D_{29} + D_{30} \quad (68)$$

As shown in panel C of Figure 1, the expression for K_{eh} is completely described only by linked diagrams. The result from this derivation also shows that K_{eh} depends only on the correlator operator of the excited state wave function. We note that since we are using Hugenholtz diagrams (as opposed to Goldstone diagrams), the expression for K_{eh} is a nonlocal operator and includes the antisymmetrized operator in its definition.[81] The loops in diagrams D_{29} and D_{30} are associated with the summation over occupied orbital indices and can be interpreted as the renormalization of the three-body and four-body operators into effective two-body particle−hole operators. As claimed in our title, eq 68 and panel C of Figure 1 present the expression of the electron−hole interaction kernel only in terms of the real-space operators, $w(1,2)$ and $g_X(1,2)$, without involving any unoccupied states.

3. RESULTS AND DISCUSSION

The derived expressions for the electron−hole interaction kernel and excitation energy were used to perform proof-of-concept calculations on molecules, clusters, and quantum dots. Practical implementation required us to make additional approximations to the derived expressions. For the proof-of-concept calculations, all the higher order diagrams were neglected and we included only the lowest order diagrams for describing the electron−hole interaction kernel. Also, for the excitation energy calculations, all contributions from diagrams that do not involve a particle−hole line were ignored. Applying these two approximations, the final expressions for the geminal-screened electron−hole interaction kernel (GSIK) and the excitation energy are given by the following expressions,

$$K_{eh}^{(I)}(1,2) = D_{28} = w(1,2)\, g_X(1,2)(1 - P_{12}) \quad (69)$$

$$\omega_X = \omega_X^0 + D_{22} + D_{23} + D_{28} \quad (70)$$

$$= \omega_X^0 + \langle i|U_h|i\rangle + \langle a|U_e|a\rangle + \langle ia|K_{eh}|ai\rangle \quad (71)$$

In this work, the uncorrelated Hamiltonian was defined as the Fock operator obtained from Hartree−Fock calculation. The transition of interest was the HOMO to LUMO transition and the single-particle (quasi) hole and electron states were defined using the HOMO and LUMO states,

$$|i\rangle \equiv |\chi_{HOMO}\rangle \quad (72)$$

$$|a\rangle \equiv |\chi_{LUMO}\rangle \quad (73)$$

The uncorrelated excitation energy was defined as the HOMO−LUMO gap,

$$\omega_X^0 = (\epsilon_{LUMO} - \epsilon_{HOMO}) \quad (74)$$

All operators U_h, U_e, and K_{eh} depend on $g_X(1,2)$, which was chosen to be an explicitly correlated Gaussian-type geminal function that depends explicitly on the electron−electron separation distance,

$$g_X(1,2) = \sum_{k=1}^{N_g} b_k^X \exp[-\gamma_k r_{12}^2] \quad (75)$$

where N_g is the number of Gaussian functions. Geminal functions have been used extensively in the past[27,73,82−85] for treating electron−electron correlation and were used in this work for construction of the correlator operator.

3.1. Excitation Energy of Water and CdSe Cluster. The excitation energy of a single water molecule was computed using eq 70, and the results were compared with EOM-CCSD[15] calculations. Both calculations were performed using 6-31G* basis, and the single-particle states were obtained from Hartree−Fock calculations. Electron−electron correlation effects for both ground and excited states were entirely treated using the explicitly correlated Gaussian-type geminal functions, and only one geminal function was used. We assumed that the correlator operator for the excited state is of a similar form to the ground state and the expansion coefficients, (b_k,γ_k), were obtained from previously published results on ground state calculations and are given in Table 3 (Appendix B).[72] Comparison of the GSIK with the EOM-CC results (Table 1) shows that the excitation energies are in good agreement with each other. We also calculated the excitation energy of a small CdSe cluster, $Cd_{20}Se_{19}$, using the LANL2DZ ECP basis and the results were compared with previously reported pseudopotential+CI (pseudopot.+CI) calculations.[86] The geminal parameters for CdSe clusters were obtained from previously reported calculations on parabolic quantum dots.[87,88] In both cases, we found that the excitation energies obtained using the geminal-screened electron−hole interaction kernel were in good agreement with previously reported results (Table 1). These results also highlight the transferability of the geminal parameters from a model potential (parabolic quantum dots in this case) to electronic structure calculations.

Table 1. Comparison of Excitation Energy (eV) for H_2O and $Cd_{20}Se_{19}$

system	this work (GSIK)	existing methods	
H_2O	8.601	8.539	(EOM-CCSD)[15]
$Cd_{20}Se_{19}$	3.139	3.096	(pseudopot.+CI)[86]

3.2. Exciton Binding Energies. In addition to calculation of the excitation energies, proof-of-concept calculations were performed on calculation of exciton binding energies. Excition binding energies are directly related to the electron−hole interaction kernel and provide a direct route to verify the quality of the derived expression. The exciton binding energies for Cd_6Se_6 and $Cd_{20}Se_{19}$ were calculated using the geminal-screened

DOI: 10.1021/acs.jctc.8b00123
J. Chem. Theory Comput. 2018, 14, 3656−3666

electron−hole interaction kernel and were compared with previously published results obtained using GW/BSE[89] and pseudopotential+CI calculations.[86] As shown in Table 2, the results from this work were found to be in good agreement with both of these methods.

Table 2. Comparison of Exciton Binding Energies (eV)

system	this work (GSIK)	previously reported	
Cd_6Se_6	3.374	3.33	(GW/BSE)[89]
$Cd_{20}Se_{19}$	0.960	1.003	(pseudopot.+CI)[86]

3.3. Extension to Spin-Resolved States. In its present form, the particle−hole excitation operator used in eq 16 is not spin-resolved. As a consequence of that, the excited state (Ψ_X) of the correlated system is not an eigenfunction of the total spin operator, $\hat{S}^2$. To extend the derivation for spin-resolved states such as singlet and triplet excited states, a modified particle−hole excitation operator with well-defined spin states must be used. For example, the singlet excitation operator is defined as[90]

$$\hat{E}_{ia}^{S=0,M_s=0} = \{a_\alpha^\dagger i_\alpha\} + \{a_\beta^\dagger i_\beta\} \tag{76}$$

where $\psi_i(\mathbf{r})$ and $\psi_a(\mathbf{r})$ refer to occupied and unoccupied spatial molecular orbitals, respectively, and α and β are the spin states. Similarly, the triplet excitation operator is defined as[90]

$$\hat{T}_{ia}^{S=1,M_s=1} = -\{a_\alpha^\dagger i_\beta\} \tag{77}$$

$$\hat{T}_{ia}^{S=1,M_s=-1} = \{a_\alpha^\dagger i_\beta\} \tag{78}$$

$$\hat{T}_{ia}^{S=1,M_s=0} = \{a_\alpha^\dagger i_\alpha\} - \{a_\beta^\dagger i_\beta\} \tag{79}$$

Using these particle−hole creation operators, the singlet and triplet excited states can be defined as

$$|\Psi_X^{S=0}\rangle = G_X^{S=0}\hat{E}_{ia}|0\rangle \tag{80}$$

$$|\Psi_X^{S=1}\rangle = G_X^{S=1}\hat{T}_{ia}|0\rangle \tag{81}$$

An important aspect of treating electron correlation in spin-resolved states is the choice of the two-body correlator operator, G. For example, in the above expression, the two-body correlator operators for the singlet and triplet states have different functional forms. This is a consequence of the different cusp conditions at the electron−electron coalescence point for spin-paired and spin-unpaired electrons. The spin dependence of the functional form near the electron−electron coalescence point has been studied extensively in the past,[91,92] and an excellent review on this topic is presented by Kong et al.[79] Future development of the GSIK method will focus on using the spin-resolved excitation operators for describing electron−hole interaction.

4. CONCLUSION

The expression for the electron−hole interaction kernel, K_{eh}, was derived without using unoccupied states. One key result from this derivation is our proof-by-construction demonstration that K_{eh} can be expressed entirely in terms of linked diagrams. By factorization of the diagrams, it was shown that contributions from all unlinked diagrams rigorously vanish from the expressions for both excitation energy and electron−hole interaction kernel. It was also shown that the electron−hole interaction kernel depends only on the electron correlator operator associated with the excited state and is independent of the level and quality of treatment of electron correlation in the ground electronic state. For the excitation energy calculations, the derivation also demonstrated the emergence of effective one-body operators that are responsible for the renormalization of the quasielectron and quasihole states. This is an important point, because in conventional GW/BSE calculations, the quasiparticle energies are obtained from the GW calculations; however, in the present derivation although GW was not performed, the renormalization of the quasiparticle states emerges in the natural course of the derivation. We note that the renormalization of quasiparticle energies also satisfies the link-cluster theorem and they are evaluated as a sum of only linked diagrams. The derived expressions were implemented and proof-of-concept calculations of excitation energies and exciton binding energies were performed for water and CdSe clusters. In all cases, the results were found to be in good agreement with the previously reported calculations. These results demonstrate the effectiveness of the geminal-screened electron−hole interaction kernel method for the efficient calculation of excited state properties in many-electron systems.

APPENDIX A

In this appendix, we present the derivation of the electron−hole interaction kernel using algebraic representation.

A.1. Evaluation of $\langle 0|WG_0|0\rangle_{FC}$

To start, we write WG_0 (eq 44) in second-quantized representation,

$$\begin{aligned} WG_0 = {} & \frac{1}{2!}\sum_{p_1q_1p_2q_2}\langle p_1p_2|\kappa_2^0|q_1q_2\rangle p_1^\dagger p_2^\dagger q_2 q_1 \\ & + \frac{1}{3!}\sum_{p_1q_1p_2q_2p_3q_3}\langle p_1p_2p_3|\kappa_3^0|q_1q_2q_3\rangle p_1^\dagger p_2^\dagger p_3^\dagger q_3 q_2 q_1 \\ & + \frac{1}{4!}\sum_{p_1q_1p_2q_2p_3q_3p_4q_4}\langle p_1p_2p_3p_4|\kappa_4^0|q_1q_2q_3q_4\rangle p_1^\dagger p_2^\dagger p_3^\dagger p_4^\dagger q_4 q_3 q_2 q_1 \end{aligned} \tag{82}$$

Using eq 33 and eq 82,

$$\begin{aligned} \langle 0|WG_0|0\rangle_{FC} = {} & \frac{1}{2!}\sum_{p_1q_1p_2q_2}\langle p_1p_2|\kappa_2^0|q_1q_2\rangle\langle 0|p_1^\dagger p_2^\dagger q_2 q_1|0\rangle_{FC} \\ & + \frac{1}{3!}\sum_{p_1q_1p_2q_2p_3q_3}\langle p_1p_2p_3|\kappa_3^0|q_1q_2q_3\rangle\langle 0|p_1^\dagger p_2^\dagger p_3^\dagger q_3 q_2 q_1|0\rangle_{FC} \\ & + \frac{1}{4!}\sum_{p_1q_1p_2q_2p_3q_3p_4q_4}\langle p_1p_2p_3p_4|\kappa_4^0|q_1q_2q_3q_4\rangle\langle 0|p_1^\dagger p_2^\dagger p_3^\dagger p_4^\dagger q_4 q_3 q_2 q_1|0\rangle_{FC} \end{aligned} \tag{83}$$

where the subscript "FC" implies that only fully contracted terms are evaluated. Inspection of the expressions show that the only nonzero terms in the above expressions must involve only occupied state indices. Including all possible nonzero contractions gives us the following expression,

$$\begin{aligned} \langle 0|WG_0|0\rangle_{FC} = {} & \frac{1}{2!}\sum_{i_1i_2}\langle i_1i_2|\kappa_2^0|i_1i_2\rangle_A \\ & + \frac{1}{3!}\sum_{i_1i_2i_3}\langle i_1i_2i_3|\kappa_3^0|i_1i_2i_3\rangle_A \\ & + \frac{1}{4!}\sum_{i_1i_2i_3i_4}\langle i_1i_2i_3i_4|\kappa_4^0|i_1i_2i_3i_4\rangle_A \end{aligned} \tag{84}$$

where subscript "A" in $\langle ...\rangle_A$ implies an antisymmetrized matrix element. Comparing to a diagrammtic representation, the

DOI: 10.1021/acs.jctc.8b00123
J. Chem. Theory Comput. 2018, 14, 3656−3666

above expression corresponds to the following closed-loop diagrams,

$$\langle 0|WG_0|0\rangle_{FC} = D_1 + D_2 + D_3 \tag{85}$$

A.2. Evaluation of $\langle 0|\{i^\dagger a\}WG_X\{a^\dagger i\}|0\rangle_{FC}$

WG_X (eq 35) in second-quantized representation is written as

$$WG_X = \frac{1}{2!}\sum_{p_1q_1p_2q_2}\langle p_1p_2|\kappa_2^X|q_1q_2\rangle p_1^\dagger p_2^\dagger q_2q_1 + \frac{1}{3!}\sum_{p_1q_1p_2q_2p_3q_3}\langle p_1p_2p_3|\kappa_3^X|q_1q_2q_3\rangle p_1^\dagger p_2^\dagger p_3^\dagger q_3q_2q_1 + \frac{1}{4!}\sum_{p_1q_1p_2q_2p_3q_3p_4q_4}\langle p_1p_2p_3p_4|\kappa_4^X|q_1q_2q_3q_4\rangle p_1^\dagger p_2^\dagger p_3^\dagger p_4^\dagger q_4q_3q_2q_1 \tag{86}$$

Using eq 33 and eq 86, we get the following expression,

$$\langle 0|\{i^\dagger a\}WG_X\{a^\dagger i\}|0\rangle_{FC} = \frac{1}{2!}\sum_{p_1q_1p_2q_2}\langle p_1p_2|\kappa_2^X|q_1q_2\rangle\langle 0|\{i^\dagger a\}p_1^\dagger p_2^\dagger q_2q_1\{a^\dagger i\}|0\rangle_{FC} + \frac{1}{3!}\sum_{p_1q_1p_2q_2p_3q_3}\langle p_1p_2p_3|\kappa_3^X|q_1q_2q_3\rangle\langle 0|\{i^\dagger a\}p_1^\dagger p_2^\dagger p_3^\dagger q_3q_2q_1\{a^\dagger i\}|0\rangle_{FC} + \frac{1}{4!}\sum_{p_1q_1p_2q_2p_3q_3p_4q_4}\langle p_1p_2p_3p_4|\kappa_4^X|q_1q_2q_3q_4\rangle\langle 0|\{i^\dagger a\}p_1^\dagger p_2^\dagger p_3^\dagger p_4^\dagger q_4q_3q_2q_1\{a^\dagger i\}|0\rangle_{FC} \tag{87}$$

To analyze the various resulting contracted terms, we introduce the following shorthand notation,

$$A = \{i^\dagger a\} \tag{88}$$

$$B = (p_1^\dagger p_2^\dagger \ldots) \tag{89}$$

$$C = (\ldots q_2q_1) \tag{90}$$

$$D = \{a^\dagger i\} \tag{91}$$

Using the above notation, the operator strings can be compactly expressed as,

$$\langle 0|\{i^\dagger a\}p_1^\dagger p_2^\dagger q_2q_1\{a^\dagger i\}|0\rangle_{FC} = \langle 0|AB_2C_2D|0\rangle_{FC} \tag{92}$$

$$\langle 0|\{i^\dagger a\}p_1^\dagger p_2^\dagger p_3^\dagger q_3q_2q_1\{a^\dagger i\}|0\rangle_{FC} = \langle 0|AB_3C_3D|0\rangle_{FC} \tag{93}$$

$$\langle 0|\{i^\dagger a\}p_1^\dagger p_2^\dagger p_3^\dagger p_4^\dagger q_4q_3q_2q_1\{a^\dagger i\}|0\rangle_{FC} = \langle 0|AB_4C_4D|0\rangle_{FC} \tag{94}$$

We note that, in all cases, the set of fully contracted terms can be factored in the following two non-overlapping subsets,

$$ABCD = \overbrace{ABCD} + \overbrace{ABCD}. \tag{95}$$

The first term in eq 95 represents pairwise contraction of only the excitation operators A and D, whereas the second term represents terms that involve all the operators. Substituting in earlier expression, we get,

$$\langle 0|ABCD|0\rangle_{FC} = \langle 0|\overbrace{AB_2C_2D} + \overbrace{AB_3C_3D} + \overbrace{AB_4C_4D}|0\rangle + \langle 0|\overbrace{AB_2C_2D} + \overbrace{AB_3C_3D} + \overbrace{AB_4C_4D}|0\rangle. \tag{96}$$

The above expression can be simplified by noting that the contraction involving the excitation operators contributes "1" to the total expression,

$$\overbrace{AD} = \delta_{ii}\delta_{aa} = 1. \tag{97}$$

The remaining contractions link all of the four different types of operators and are collectively referred to as the linked terms. This implies the following simplification,

$$\langle 0|ABCD|0\rangle_{FC} = \langle 0|BC|0\rangle_{FC} + \langle 0|ABCD|0\rangle_{L} \tag{98}$$

where subscript "L" implies only *linked*, fully contracted terms. Because $\langle 0|BC|0\rangle_{FC}$ does not contain any terms from excitation operators, it is similar to the expression of $\langle 0|WG_0|0\rangle$ derived earlier. Consequently, we can write the expression for $\langle 0|\{i^\dagger a\}WG_n\{a^\dagger i\}|0\rangle_{FC}$ as

$$\langle 0|\{i^\dagger a\}WG_n\{a^\dagger i\}|0\rangle_{FC} = \langle 0|WG_n|0\rangle_{FC} + \langle 0|\{i^\dagger a\}WG_n\{a^\dagger i\}|0\rangle_{L} \tag{99}$$

Comparing to the diagrammtic representation, the fully contracted terms can be compactly represented as

$$\langle 0|\{i^\dagger a\}WG_n\{a^\dagger i\}|0\rangle_{FC} = D_4 + \ldots + D_{18} \tag{100}$$

APPENDIX B

The b and γ values used in this work are presented in Table 3.

Table 3. b and γ Values (a.u.) Used in GSIK Method[a]

system	b	γ
H_2O	0.186766	0.557658
Cd_6Se_6	0.128975	0.052184
$Cd_{20}Se_{19}$	0.867863	0.010425

[a]The form of the correlation operator used in this work is of similar form to the ground state correlation operator presented in earlier work.[72].

ASSOCIATED CONTENT

Supporting Information

The Supporting Information is available free of charge on the ACS Publications website at DOI: 10.1021/acs.jctc.8b00123.

Description of the Hugenholtz diagrams, its connection to Goldstone diagrams, and derivation of matrix elements (PDF)

AUTHOR INFORMATION

Corresponding Author

*E-mail: archakra@syr.edu.

ORCID

Arindam Chakraborty: 0000-0003-2710-0637

Funding

This material is based upon work supported by the National Science Foundation under Grant No. CHE-1349892. This work used the Extreme Science and Engineering Discovery Environment (XSEDE), which is supported by National Science Foundation grant number ACI-1053575. We are also grateful to Syracuse University for additional computational and financial support.

Notes

The authors declare no competing financial interest.

REFERENCES

(1) Onida, G.; Reining, L.; Rubio, A. Electronic excitations: density-functional versus many-body Green's-function approaches. *Rev. Mod. Phys.* **2002**, *74*, 601−659.

(2) Guareschi, R.; Floris, F.; Amovilli, C.; Filippi, C. Solvent effects on excited-state structures: A quantum Monte Carlo and density functional study. *J. Chem. Theory Comput.* **2014**, *10*, 5528−5537.

(3) Deotare, P.; Chang, W.; Hontz, E.; Congreve, D.; Shi, L.; Reusswig, P.; Modtland, B.; Bahlke, M.; Lee, C.; Willard, A.; Bulovic,

DOI: 10.1021/acs.jctc.8b00123
J. Chem. Theory Comput. 2018, 14, 3656−3666

V.; Van Voorhis, T.; Baldo, M. Nanoscale transport of charge-transfer states in organic donor-acceptor blends. *Nat. Mater.* **2015**, *14*, 1130−1134.
(4) Chang, W.; Congreve, D.; Hontz, E.; Bahlke, M.; McMahon, D.; Reineke, S.; Wu, T.; Bulovic, V.; Van Voorhis, T.; Baldo, M. Spin-dependent charge transfer state design rules in organic photovoltaics. *Nat. Commun.* **2015**, *6*, 6415.
(5) Yang, Z.-H.; Sottile, F.; Ullrich, C. Simple screened exact-exchange approach for excitonic properties in solids. *Phys. Rev. B: Condens. Matter Mater. Phys.* **2015**, *92*, 035202.
(6) Rohlfing, M.; Louie, S. G. Electron-hole excitations and optical spectra from first principles. *Phys. Rev. B: Condens. Matter Mater. Phys.* **2000**, *62*, 4927−4944.
(7) Melnikov, D. V.; Chelikowsky, J. R. Electron affinities and ionization energies in Si and Ge nanocrystals. *Phys. Rev. B: Condens. Matter Mater. Phys.* **2004**, *69*, 113305.
(8) Tiago, M. L.; Chelikowsky, J. R. First-principles GW-BSE excitations in organic molecules. *Solid State Commun.* **2005**, *136*, 333−337.
(9) Tiago, M. L.; Idrobo, J. C.; Öğüt, S.; Jellinek, J.; Chelikowsky, J. R. Electronic and optical excitations in Ag_n clusters (n = 1−8): Comparison of density-functional and many-body theories. *Phys. Rev. B: Condens. Matter Mater. Phys.* **2009**, *79*, 155419.
(10) Hung, L.; da Jornada, F. H.; Souto-Casares, J.; Chelikowsky, J. R.; Louie, S. G.; Öğüt, S. Excitation spectra of aromatic molecules within a real-space *GW*-BSE formalism: Role of self-consistency and vertex corrections. *Phys. Rev. B: Condens. Matter Mater. Phys.* **2016**, *94*, 085125.
(11) Bruneval, F.; Hamed, S.; Neaton, J. A systematic benchmark of the ab initio Bethe-Salpeter equation approach for low-lying optical excitations of small organic molecules. *J. Chem. Phys.* **2015**, *142*, 244101.
(12) Benedict, L.; Puzder, A.; Williamson, A.; Grossman, J.; Galli, G.; Klepeis, J.; Raty, J.-Y.; Pankratov, O. Calculation of optical absorption spectra of hydrogenated Si clusters: Bethe-Salpeter equation versus time-dependent local-density approximation. *Phys. Rev. B: Condens. Matter Mater. Phys.* **2003**, *68*, 085310.
(13) Rocca, D.; Vörös, M.; Gali, A.; Galli, G. Ab initio optoelectronic properties of silicon nanoparticles: Excitation energies, sum rules, and Tamm-Dancoff approximation. *J. Chem. Theory Comput.* **2014**, *10*, 3290−3298.
(14) Ou, Q.; Subotnik, J. E. Comparison between the BetheSalpeter Equation and Configuration Interaction Approaches for Solving a Quantum Chemistry Problem: Calculating the Excitation Energy for Finite 1D Hubbard Chains. *J. Chem. Theory Comput.* **2018**, *14*, 527−542.
(15) Shavitt, I.; Bartlett, R. *Many-Body Methods in Chemistry and Physics: MBPT and Coupled-Cluster Theory*; Cambridge Molecular Science; Cambridge University Press, 2009.
(16) Furche, F. Developing the random phase approximation into a practical post-Kohn-Sham correlation model. *J. Chem. Phys.* **2008**, *129*, 114105.
(17) Refaely-Abramson, S.; Baer, R.; Kronik, L. Fundamental and excitation gaps in molecules of relevance for organic photovoltaics from an optimally tuned range-separated hybrid functional. *Phys. Rev. B: Condens. Matter Mater. Phys.* **2011**, *84*, 075144.
(18) Refaely-Abramson, S.; Sharifzadeh, S.; Govind, N.; Autschbach, J.; Neaton, J.; Baer, R.; Kronik, L. Quasiparticle spectra from a nonempirical optimally tuned range-separated hybrid density functional. *Phys. Rev. Lett.* **2012**, *109*, 226405.
(19) Van Setten, M.; Caruso, F.; Sharifzadeh, S.; Ren, X.; Scheffler, M.; Liu, F.; Lischner, J.; Lin, L.; Deslippe, J.; Louie, S.; Yang, C.; Weigend, F.; Neaton, J.; Evers, F.; Rinke, P. GW100: Benchmarking G_0W_0 for Molecular Systems. *J. Chem. Theory Comput.* **2015**, *11*, 5665−5687.
(20) Varley, J.; Schleife, A. Bethe-Salpeter calculation of optical-absorption spectra of In_2O_3 and Ga_2O_3. *Semicond. Sci. Technol.* **2015**, *30*, 024010.
(21) Chen, G.; Voora, V.; Agee, M.; Balasubramani, S.; Furche, F. Random-Phase Approximation Methods. *Annu. Rev. Phys. Chem.* **2017**, *68*, 421−445.
(22) Dreuw, A.; Head-Gordon, M. Single-Reference ab Initio Methods for the Calculation of Excited States of Large Molecules. *Chem. Rev.* **2005**, *105*, 4009−4037.
(23) Casida, M.; Huix-Rotllant, M. Progress in Time-Dependent Density-Functional Theory. *Annu. Rev. Phys. Chem.* **2012**, *63*, 287−323.
(24) Ullrich, C. A. *Time-dependent density-functional theory: concepts and applications*; Oxford University Press: Oxford, U.K., 2011.
(25) Marques, M. A.; Maitra, N. T.; Nogueira, F. M.; Gross, E. K.; Rubio, A. *Fundamentals of time-dependent density functional theory*; Springer Science & Business Media, 2012; Vol. *837*.
(26) Maitra, N. Perspective: Fundamental aspects of time-dependent density functional theory. *J. Chem. Phys.* **2016**, *144*, 220901.
(27) Nichols, B.; Rassolov, V. Description of electronic excited states using electron correlation operator. *J. Chem. Phys.* **2013**, *139*, 104111.
(28) Govoni, M.; Galli, G. Large Scale GW Calculations. *J. Chem. Theory Comput.* **2015**, *11*, 2680−2696.
(29) Scherpelz, P.; Govoni, M.; Hamada, I.; Galli, G. Implementation and Validation of Fully Relativistic GW Calculations: Spin-Orbit Coupling in Molecules, Nanocrystals, and Solids. *J. Chem. Theory Comput.* **2016**, *12*, 3523−3544.
(30) Brawand, N. P.; Vörös, M.; Govoni, M.; Galli, G. Generalization of Dielectric-Dependent Hybrid Functionals to Finite Systems. *Phys. Rev. X* **2016**, *6*, 041002.
(31) Simons, J.; Smith, W. Theory of electron affinities of small molecules. *J. Chem. Phys.* **1973**, *58*, 4899.
(32) Smith, W.; Chen, T.-T.; Simons, J. Theoretical studies of molecular ions. Vertical ionization potentials of hydrogen fluoride. *J. Chem. Phys.* **1974**, *61*, 2670−2674.
(33) Griffing, K.; Simons, J. Theoretical studies of molecular ions. The ionization potential and electron affinity of BH. *J. Chem. Phys.* **1975**, *62*, 535−540.
(34) Andersen, E.; Simons, J. A calculation of the electron affinity of the lithium molecule. *J. Chem. Phys.* **1976**, *64*, 4548−4550.
(35) Chen, T.-T.; Smith, W.; Simons, J. Theoretical studies of molecular ions. Vertical ionization potentials of the nitrogen molecule. *Chem. Phys. Lett.* **1974**, *26*, 296−300.
(36) Simons, J. Response of a Molecule to Adding or Removing an Electron. *Adv. Quantum Chem.* **2005**, *50*, 213−233.
(37) Hirata, S.; Hermes, M.; Simons, J.; Ortiz, J. General-order many-body greens function method. *J. Chem. Theory Comput.* **2015**, *11*, 1595−1606.
(38) Cederbaum, L.; Hohlneicher, G.; Peyerimhoff, S. Calculation of the vertical ionization potentials of formaldehyde by means of perturbation theory. *Chem. Phys. Lett.* **1971**, *11*, 421−424.
(39) Cederbaum, L. Direct calculation of ionization potentials of closed-shell atoms and molecules. *Theor. Chim. Acta* **1973**, *31*, 239−260.
(40) Cederbaum, L.; Von Niessen, W. Direct calculation of ionization potentials of atoms and molecules: application to Ne. *Chem. Phys. Lett.* **1974**, *24*, 263−266.
(41) Cederbaum, L. One-body Green's function for atoms and molecules: Theory and application. *J. Phys. B: At. Mol. Phys.* **1975**, *8*, 290−303.
(42) Von Niessen, W.; Cederbaum, L.; Kraemer, W. The electronic structure of molecules by a many-body approach. I. Ionization potentials and one-electron properties of benzene. *J. Chem. Phys.* **1976**, *65*, 1378−1386.
(43) Yeager, D.; McKoy, V. An equations of motion approach for open shell systems. *J. Chem. Phys.* **1975**, *63*, 4861−4869.
(44) Herman, M.; Yeager, D.; Freed, K.; McKoy, V. Critical analysis of equations-of-motion-Green's function method: Ionization potentials of N_2. *Chem. Phys. Lett.* **1977**, *46*, 1−7.
(45) Freed, K.; Yeager, D. A wavefunction approach to equations of motion-Green's function methods. *Chem. Phys.* **1977**, *22*, 401−414.

DOI: 10.1021/acs.jctc.8b00123
J. Chem. Theory Comput. 2018, 14, 3656−3666

(46) Freed, K.; Herman, M.; Yeager, D. Critical comparison between equation of motion-green's function methods and configuration interaction methods: Analysis of methods and applications. *Phys. Scr.* **1980**, *21*, 242−250.
(47) Herman, M.; Freed, K.; Yeager, D. Critical test of equation-of-motion-Green's function methods. I. Theory of higher order terms. *J. Chem. Phys.* **1980**, *72*, 602−610.
(48) Herman, M.; Freed, K.; Yeager, D.; Liu, B. Critical test of equation-of-motion-Green's function methods. II. Comparison with configuration interaction results. *J. Chem. Phys.* **1980**, *72*, 611−620.
(49) Lynch, D.; Herman, M.; Yeager, D. Excited state properties from the equations of motion method. Application of the MCTDHF-MCRPA to the dipole moments and oscillator strengths of the AΠ1, aΠ′3, aΣ′3$^+$, and dΔ3 low-lying valence states of CO. *Chem. Phys.* **1982**, *64*, 69−81.
(50) Liang, L.; Yeager, D. L. The complex scaled multiconfigurational time-dependent Hartree-Fock method for studying resonant states: Application to the 2 s^2 He Feshbach resonance. *J. Chem. Phys.* **2014**, *140*, 094305.
(51) Kato, T. On the eigenfunctions of many-particle systems in quantum mechanics. *Communications on Pure and Applied Mathematics* **1957**, *10*, 151−177.
(52) Nightingale, M. P.; Umrigar, C. J. *Quantum Monte Carlo methods in physics and chemistry*; Springer, 1998; Vol. *525*.
(53) Hammond, B. L.; Lester, W. A.; Reynolds, P. J. *Monte Carlo methods in ab initio quantum chemistry*; World Scientific: Singapore, 1994; Vol. *2*.
(54) Boys, S.; Handy, N. A condition to remove the indeterminacy in interelectronic correlation functions. *Proc. R. Soc. London, Ser. A* **1969**, *309*, 209−220.
(55) Boys, S.; Handy, N. The determination of energies and wavefunctions with full electronic correlation. *Proc. R. Soc. London, Ser. A* **1969**, *310*, 43−61.
(56) Slater, J. C. Central Fields and Rydberg Formulas in Wave Mechanics. *Phys. Rev.* **1928**, *31*, 333−343.
(57) Slater, J. C. The Normal State of Helium. *Phys. Rev.* **1928**, *32*, 349−360.
(58) Hylleraas, E. Neue Berechnung der Energie des Heliums im Grundzustande, sowie des tiefsten Terms von Ortho-Helium. *Eur. Phys. J. A* **1929**, *54*, 347−366.
(59) Hylleraas, E. Über den Grundterm der Zweielektronenprobleme von H, He, Li+, Be++ usw. *Eur. Phys. J. A* **1930**, *65*, 209−225.
(60) Ten-no, S. A feasible transcorrelated method for treating electronic cusps using a frozen Gaussian geminal. *Chem. Phys. Lett.* **2000**, *330*, 169−174.
(61) Ten-no, S. Three-electron integral evaluation in the trans-correlated method using a frozen Gaussian geminal. *Chem. Phys. Lett.* **2000**, *330*, 175−179.
(62) Ten-no, S.; Hino, O. New Transcorrelated Method Improving the Feasibility of Explicitly Correlated Calculations. *Int. J. Mol. Sci.* **2002**, *3*, 459−474.
(63) Swalina, C.; Pak, M.; Chakraborty, A.; Hammes-Schiffer, S. Explicit dynamical electron-proton correlation in the nuclear-electronic orbital framework. *J. Phys. Chem. A* **2006**, *110*, 9983−9987.
(64) Chakraborty, A.; Pak, M.; Hammes-Schiffer, S. Inclusion of explicit electron-proton correlation in the nuclear-electronic orbital approach using Gaussian-type geminal functions. *J. Chem. Phys.* **2008**, *129*, 014101.
(65) Sirjoosingh, A.; Pak, M. V.; Swalina, C.; Hammes-Schiffer, S. Reduced explicitly correlated Hartree-Fock approach within the nuclear-electronic orbital framework: Applications to positronic molecular systems. *J. Chem. Phys.* **2013**, *139*, 034103.
(66) Sirjoosingh, A.; Pak, M. V.; Swalina, C.; Hammes-Schiffer, S. Reduced explicitly correlated Hartree-Fock approach within the nuclear-electronic orbital framework: Theoretical formulation. *J. Chem. Phys.* **2013**, *139*, 034102.
(67) Brorsen, K. R.; Sirjoosingh, A.; Pak, M. V.; Hammes-Schiffer, S. Nuclear-electronic orbital reduced explicitly correlated Hartree-Fock approach: Restricted basis sets and open-shell systems. *J. Chem. Phys.* **2015**, *142*, 214108.
(68) Sirjoosingh, A.; Pak, M. V.; Brorsen, K. R.; Hammes-Schiffer, S. Quantum treatment of protons with the reduced explicitly correlated Hartree-Fock approach. *J. Chem. Phys.* **2015**, *142*, 214107.
(69) Elward, J. M.; Thallinger, B.; Chakraborty, A. Calculation of electron-hole recombination probability using explicitly correlated Hartree-Fock method. *J. Chem. Phys.* **2012**, *136*, 124105.
(70) Elward, J. M.; Hoja, J.; Chakraborty, A. Variational solution of the congruently transformed Hamiltonian for many-electron systems using a full-configuration-interaction calculation. *Phys. Rev. A: At., Mol., Opt. Phys.* **2012**, *86*, 062504.
(71) Bayne, M. G.; Drogo, J.; Chakraborty, A. Infinite-order diagrammatic summation approach to the explicitly correlated congruent transformed Hamiltonian. *Phys. Rev. A: At., Mol., Opt. Phys.* **2014**, *89*, 032515.
(72) Bayne, M. G.; Uchida, Y.; Eller, J.; Daniels, C.; Chakraborty, A. Construction of explicitly correlated geminal-projected particle-hole creation operators for many-electron systems using the diagrammatic factorization approach. *Phys. Rev. A: At., Mol., Opt. Phys.* **2016**, *94*, 052504.
(73) Varganov, S. A.; Martínez, T. J. Variational geminal-augmented multireference self-consistent field theory: Two-electron systems. *J. Chem. Phys.* **2010**, *132*, 054103.
(74) Cassam-Chenai, P.; Rassolov, V. The electronic mean field configuration interaction method: III the p-orthogonality constraint. *Chem. Phys. Lett.* **2010**, *487*, 147−152.
(75) Cagg, B. A.; Rassolov, V. A. SSpG: A strongly orthogonal geminal method with relaxed strong orthogonality. *J. Chem. Phys.* **2014**, *141*, 164112.
(76) Jeszenszki, P.; Rassolov, V.; Surján, P. R.; Szabados, Á Local spin from strongly orthogonal geminal wavefunctions. *Mol. Phys.* **2015**, *113*, 249−259.
(77) Klopper, W.; Manby, F. R.; Ten-No, S.; Valeev, E. F. R12 methods in explicitly correlated molecular electronic structure theory. *Int. Rev. Phys. Chem.* **2006**, *25*, 427−468.
(78) Tenno, S.; Noga, J. Explicitly correlated electronic structure theory from R12/F12 anstze. *WIRs Comput. Mol. Sci.* **2012**, *2*, 114−125.
(79) Kong, L.; Bischoff, F. A.; Valeev, E. F. Explicitly Correlated R12/F12 Methods for Electronic Structure. *Chem. Rev.* **2012**, *112*, 75−107.
(80) Hättig, C.; Klopper, W.; Köhn, A.; Tew, D. P. Explicitly Correlated Electrons in Molecules. *Chem. Rev.* **2012**, *112*, 4−74.
(81) See Supporting Information. Contains the Hugenholtz diagrams review.
(82) Szalewicz, K.; Jeziorski, B. Explicitly-correlated Gaussian geminals in electronic structure calculations. *Mol. Phys.* **2010**, *108*, 3091−3103.
(83) Mitroy, J.; Bubin, S.; Horiuchi, W.; Suzuki, Y.; Adamowicz, L.; Cencek, W.; Szalewicz, K.; Komasa, J.; Blume, D.; Varga, K. Theory and application of explicitly correlated Gaussians. *Rev. Mod. Phys.* **2013**, *85*, 693−749.
(84) Bubin, S.; Pavanello, M.; Tung, W.-C.; Sharkey, K. L.; Adamowicz, L. Born-Oppenheimer and Non-Born-Oppenheimer, Atomic and Molecular Calculations with Explicitly Correlated Gaussians. *Chem. Rev.* **2013**, *113*, 36−79.
(85) Mitroy, J.; Bubin, S.; Horiuchi, W.; Suzuki, Y.; Adamowicz, L.; Cencek, W.; Szalewicz, K.; Komasa, J.; Blume, D.; Varga, K. Theory and application of explicitly correlated Gaussians. *Rev. Mod. Phys.* **2013**, *85*, 693−749.
(86) Wang, L.-W.; Zunger, A. Pseudopotential calculations of nanoscale CdSe quantum dots. *Phys. Rev. B: Condens. Matter Mater. Phys.* **1996**, *53*, 9579−9582.
(87) Elward, J.; Chakraborty, A. Effect of dot size on exciton binding energy and electron-hole recombination probability in CdSe quantum dots. *J. Chem. Theory Comput.* **2013**, *9*, 4351−4359.

DOI: 10.1021/acs.jctc.8b00123
J. Chem. Theory Comput. 2018, 14, 3656−3666

(88) Elward, J.; Chakraborty, A. Effect of heterojunction on exciton binding energy and electron-hole recombination probability in CdSe/ZnS quantum dots. *J. Chem. Theory Comput.* **2015**, *11*, 462−471.
(89) Noguchi, Y.; Sugino, O.; Nagaoka, M.; Ishii, S.; Ohno, K. A GW +Bethe-Salpeter calculation on photoabsorption spectra of $(CdSe)_3$ and $(CdSe)_6$ clusters. *J. Chem. Phys.* **2012**, *137*, 024306.
(90) Helgaker, T.; Jorgensen, P.; Olsen, J. *Molecular Electronic-structure Theory*; Wiley, 2008.
(91) Thakkar, A. J. The higher order electronelectron coalescence condition for the intracule function for states of maximum spin multiplicity. *J. Chem. Phys.* **1986**, *84*, 6830−6832.
(92) Huang, C.-J.; Filippi, C.; Umrigar, C. J. Spin contamination in quantum Monte Carlo wave functions. *J. Chem. Phys.* **1998**, *108*, 8838−8847.

DOI: 10.1021/acs.jctc.8b00123
J. Chem. Theory Comput. 2018, 14, 3656−3666